

## ROBUSTNESS OF STOCHASTIC CHEMICAL REACTION NETWORKS TO EXTRINSIC NOISE: THE ROLE OF DEFICIENCY\*

ETHAN LEVIEN<sup>†</sup> AND PAUL C. BRESSLOFF<sup>†</sup>

**Abstract.** The biochemical systems inside a living cell are able to reliably perform complex tasks while subjected to various sources of noise. In this study we consider stochastic models of biochemical networks evolving in the presence of dynamic random environments. These environments are themselves modeled as chemical reaction networks so that the full system can be viewed as a multiscale chemical reaction network. The multiscale structure arises from the fact that the environment and the internal system may operate on different timescales. While previous results in chemical reaction network theory have established that certain dynamic behavior can be ruled out when a topological parameter, known as the network deficiency, is zero, these results fail to capture the behavior that can be observed in multiscale networks. We demonstrate that the deficiency of the network has implications for how robust it is to environmental noise. We then show how our results can be used to prove that correlations in a population of chemical reaction networks in a random environment vanish given certain topological constraints.

**Key words.** chemical reaction networks, deficiency, robustness, multiscale, stochastic gene expression, environmental noise

**AMS subject classifications.** 92C42, 92C45, 60J28

**DOI.** 10.1137/17M1146609

**1. Introduction.** The question of how biochemical systems function while subjected to various sources of noise has attracted significant attention in both the theoretical and experimental literature [17, 31, 9]. When analyzing these systems it is typical to consider two categories of randomness: intrinsic noise arising from stochasticity within the cellular system and extrinsic noise due to external inputs, such as changes in the environment [20, 28, 11, 4]. In many applications extrinsic and intrinsic processes operate on different timescales, leading to a system that has multiscale dynamics [27, 10, 21]. For example, in models of gene expression the switching of the gene between an active and an inactive state can be interpreted as a source of extrinsic noise, while the fluctuations in the concentration of the gene product is treated as intrinsic noise. (In some contexts these noise sources are both intrinsic [28]. Technically, the difference between intrinsic and extrinsic depends on the physical source of the noise.) If the production rate when the gene is in the active state is large, the intrinsic noise will be weak. On the other hand, the activation/deactivation rates of the gene may be only moderate, leading to a separation of timescales [9, 31].

For systems with only intrinsic noise occurring on a single timescale, or equivalently, *classically scaled systems*, the problem of determining conditions under which chemical systems admits stable behavior over long periods of time has been well studied [1]. These systems are generally modeled by continuous time Markov chains with a single scaling parameter known as the *system-size* [15]. Given some relatively mild assumptions on the network structure, the random evolution is well approximated

---

\*Received by the editors September 7, 2017; accepted for publication (in revised form) December 11, 2017; published electronically DATE.

<http://www.siam.org/journals/mms/x-x/M114660.html>

**Funding:** The second author was supported by the National Science Foundation (DMS-1613048).

<sup>†</sup>Department of Mathematics, University of Utah, Salt Lake City, UT 84112 (levien@math.utah.edu, bressloff@math.utah.edu).

by a deterministic system of ODEs when the system-size becomes large [24, 25, 32]. These ODEs are known as reaction rate or kinetic equations. There has been a particular interest in classifying networks for which the behavior over long periods of time is relatively *tame* [14, 30]. For the stochastic model, this means that the stationary density is Poisson like, while for the deterministic approximation, it means that a positive equilibrium is approached for all initial conditions [1]. A fundamental result in the theory of chemical reaction networks (CRNs) is the *deficiency zero theorem*, which rules out more exotic dynamical behavior for networks satisfying a topological condition [2]. This theorem suggests that the class of networks with tame behavior over long periods of time is much larger than one would expect given that such systems are highly nonlinear [30]. However, from a mathematical perspective this is not so surprising; the relevant topological parameter is the *deficiency*, which is a measure of how much information is lost by transforming the nonlinear system to a linear one [29].

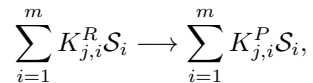
In the present study we consider the role of deficiency in the long-time behavior of multiscale CRNs. The multiscale structure comes from partitioning the network into an extrinsic part, which operates on a slow timescale, and an intrinsic part operating on a relatively fast timescale. We take the abundances of species in the system to be very large so that the intrinsic noise vanishes, allowing us to study the effects of extrinsic noise. Our main result is that if the deficiency of the entire system, including the population and the environment, is zero, the concentrations of species in the population converge almost surely to an equilibrium for suitable initial conditions. This establishes that certain deficiency zero networks are not sensitive to external noise. While there are many studies concerning both stochastic and deterministic models of deficiency zero networks, there has been little work towards an understanding of how the deficiency interacts with multiscale dynamics. Moreover, we extend our theory to a population level description of CRNs, which to our knowledge has not been discussed in the CRN theory literature.

The paper is organized as follows. In section 2 we present the necessary background material for the remainder of the paper. In section 3 we present examples of CRNs and examine their multiscale dynamics. In section 4 we generalize the observations obtained from the examples and prove theorems concerning the long-time behavior of deficiency zero and positive deficiency networks. In section 5 we introduce a population level interpretation of a CRN and show how the result from section 4 can be used to study correlations of CRNs evolving in a common environment.

**2. Chemical reaction networks.** The mathematical framework we will use to formulate the ideas in this paper is known as CRN theory [2, 16]. Within this theory one distinguishes the topology of a chemical system from the dynamics. The former tells us *what* types of reactions occur, meaning which chemical species react and what happens when they do, while the latter tells us *when* these reactions occur, meaning how the occurrences of these reactions are distributed in time.

**2.1. Topological aspects.** We begin our presentation with a purely topological definition [16]: A CRN is a tuple  $(\mathcal{S}, \mathcal{C}, \mathcal{R})$ . The first element  $\mathcal{S} = (\mathcal{S}_1, \mathcal{S}_2, \dots, \mathcal{S}_m)$  is a finite set of *species*. For specific CRNs, the elements of  $\mathcal{S}$  are often denoted by capital letters (e.g.,  $\mathcal{S}_1 = A$ ,  $\mathcal{S}_2 = B$ ,  $\mathcal{S}_3 = C, \dots$ ), or the names of chemicals (e.g.,  $\mathcal{S}_1 = RNA$ ,  $\mathcal{S}_2 = DNA$ ,  $\mathcal{S}_3 = mRNA, \dots$ ).  $\mathcal{C}$  is a set of linear combinations of elements in  $\mathcal{S}$  called *complexes*: if  $\mathcal{C} \in \mathcal{C}$ , then  $\mathcal{C} = \sum_{i=1}^m K_i \mathcal{S}_i$ , where  $K_i$  are positive constants. It follows that each complex can be identified with a vector in *species space* given by  $\mathcal{K} = (K_1, \dots, K_m) \in \mathbb{N}_+^m \equiv \mathcal{C}$ . If  $\mathcal{S}_i$  is the *i*th species in  $\mathcal{S}$ ,

then  $K_i$  represents the number of species  $S_i$  in the complex  $K$ . Finally,  $\mathcal{R}$  is a set of single step *reactions*. Each reaction can be thought of as a directed edge between two complexes. That is, the  $j$ th reaction is of the form



where the *stoichiometry* of the reaction is given by the complexes  $\mathbf{K}_j^R = (K_{j,1}^R, \dots, K_{j,m}^R)^T$  and  $\mathbf{K}_j^P = (K_{j,1}^P, \dots, K_{j,m}^P)^T$ , specifying the *reactants* and *products*, respectively. Together, the set of reactions defines a graph on the set of complexes. The vector  $\mathbf{K}_j = \mathbf{K}_j^P - \mathbf{K}_j^R$  is known as the *reaction direction* and describes the direction in the state space in which the  $j$ th reaction pushes the systems. More precisely, when the  $j$ th reaction occurs the number of  $S_i$  molecules changes by  $K_{j,i}$ . The matrix

$$\mathbf{K} = [ \mathbf{K}_1 \quad \mathbf{K}_2 \quad \cdots \quad \mathbf{K}_{|\mathcal{R}|} ]$$

is known as the *stoichiometric matrix* associated with a CRN.

**2.1.1. Example: Catalysis.** As an illustration of the above notation, consider the network whose reactions are given by



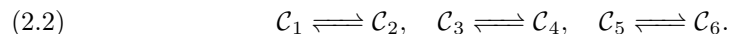
The corresponding graph describes a CRN with species  $\mathcal{S} = \{A, B, C, D\}$ . Notice that for each reaction the reverse reaction, obtained by exchanging the roles of products and reactants, is also in the network. For this reason we say that the network (2.1) is *reversible*. The set of complexes corresponding to this network is

$$\begin{aligned} \mathcal{C}_1 &= C + A, & \mathcal{C}_2 &= B + C, & \mathcal{C}_3 &= D + B, \\ \mathcal{C}_4 &= D + A, & \mathcal{C}_5 &= C, & \mathcal{C}_6 &= D, \end{aligned}$$

and the stoichiometric matrix for the six one-step reactions is

$$\mathbf{K} = \begin{bmatrix} -1 & 1 & 1 & -1 & 0 & 0 \\ 1 & -1 & -1 & 1 & 0 & 0 \\ 0 & 0 & 0 & 0 & -1 & 1 \\ 0 & 0 & 0 & 0 & 1 & -1 \end{bmatrix}.$$

In CRN theory it is sometimes useful to view a CRN as a graph on the space of complexes, ignoring the species level structure [16]. In the present context, this graph is given by



If we want to study this graph algebraically, the stoichiometric matrix  $\mathbf{K}$  becomes less relevant. Instead, we are interested in the *incidence matrix*,

$$\mathbf{J} = \begin{bmatrix} -1 & +1 & 0 & 0 & 0 & 0 \\ +1 & -1 & 0 & 0 & 0 & 0 \\ 0 & 0 & -1 & +1 & 0 & 0 \\ 0 & 0 & +1 & -1 & 0 & 0 \\ 0 & 0 & 0 & 0 & -1 & +1 \\ 0 & 0 & 0 & 0 & +1 & -1 \end{bmatrix}.$$

In the incidence matrix each column represents an edge and  $-1$  and  $+1$  are placed in indices of vertices representing the source and destination of the edge, respectively. In contrast to the stoichiometric matrix, which describes how reactions act on the space of species, the incidence matrix describes how reactions act on the space of complexes. The relationship between these objects plays a significant role in CRN theory. In particular, many results for both deterministic and stochastic systems require restrictions on the quantity

$$(2.3) \quad \delta = \dim(\ker(\mathbf{K})) - \dim(\ker(\mathbf{J})),$$

known as the *deficiency* of a CRN.<sup>1</sup> A straightforward calculation reveals the deficiency of (2.1) is one. More specifically, the null space of  $\mathbf{K}$  is spanned by the vectors

$$\begin{bmatrix} 1 \\ 1 \\ 0 \\ 0 \\ 0 \\ 0 \end{bmatrix}, \begin{bmatrix} 0 \\ 0 \\ 1 \\ 1 \\ 0 \\ 0 \end{bmatrix}, \begin{bmatrix} 0 \\ 0 \\ 0 \\ 0 \\ 1 \\ 1 \end{bmatrix}, \begin{bmatrix} 1 \\ 0 \\ 1 \\ 0 \\ 0 \\ 0 \end{bmatrix},$$

so  $\dim(\ker(\mathbf{K})) = 4$ , whereas the null space of  $\mathbf{J}$  is spanned by the vectors

$$\begin{bmatrix} 1 \\ 1 \\ 0 \\ 0 \\ 0 \\ 0 \end{bmatrix}, \begin{bmatrix} 0 \\ 0 \\ 1 \\ 1 \\ 0 \\ 0 \end{bmatrix}, \begin{bmatrix} 0 \\ 0 \\ 0 \\ 0 \\ 1 \\ 1 \end{bmatrix},$$

so  $\dim(\ker(\mathbf{J})) = 3$ .

The motivation for defining  $\delta$  can be understood as follows. First, it is well known that  $\ker(\mathbf{J})$  is equal to the number of distinct, undirected, closed cycles in the corresponding graph. Second, any linear combination of reaction directions can be interpreted as a sequence of points in the *state space*  $\mathbb{N}^m$ . This is the space in which the dynamic models introduced in the next section will evolve. From this we see that  $\ker(\mathbf{K})$  represents the number of distinct, undirected reaction cycles in state space. Of course each directed cycle in the reaction graph can be realized as a cycle in the state space, but it is possible that there are cycles of reactions realized in state space that do not appear in the reaction graph. This leads to the following interpretation of  $\delta$ : the deficiency is the number of distinct reaction cycles in  $\mathbb{R}^m$  that cannot be realized as distinct cycles in the graphical representation in terms of complexes [29].

Returning to the network (2.1), we see that the sequence of reactions



is a cycle, which is illustrated in Figure 2.1. On the other hand, in complex space this cycle corresponds to  $\{\mathcal{C}_1 \longrightarrow \mathcal{C}_2, \mathcal{C}_3 \longrightarrow \mathcal{C}_4\}$ , which is not a connected cycle in the graph (2.2). Note that  $\{C + A \longrightarrow B + C, D + B \longrightarrow A + D\}$  is also a cycle

<sup>1</sup>See [16] for alternative definitions. For all the networks considered in this paper these definitions are equivalent.

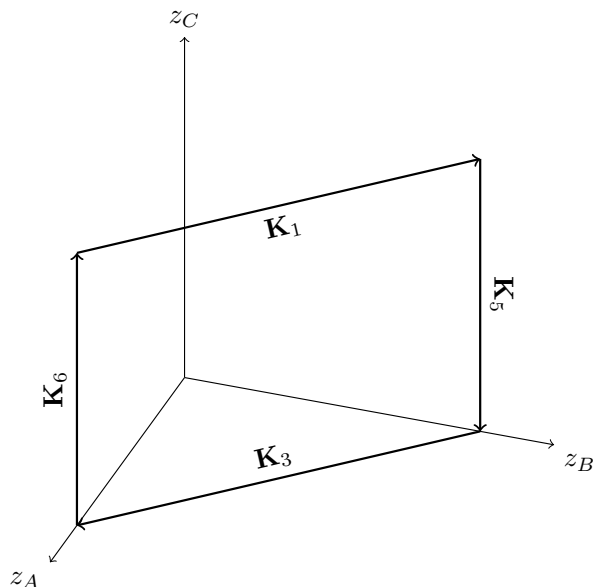


FIG. 2.1. A cycle of reactions in the network (2.1) that is not realized in the graph (2.2). We have projected  $\mathbb{R}^4$  onto  $\mathbb{R}^3$ , eliminating the  $x_D$  axis.

that is not realized in the graph (2.2); however, this is not an independent cycle in  $\mathbb{R}^4$  because it coincides with the cycle



which is realized in complex space as  $\{\mathcal{C}_1 \longrightarrow \mathcal{C}_2, \mathcal{C}_2 \longrightarrow \mathcal{C}_1\}$ .

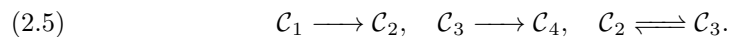
**2.1.2. Example: Two-state gene regulatory network.** An important CRN models a simple gene regulatory network shown in Figure 2.2. This consists of a gene that can be in either an active state (represented by the presence of a  $C$  “molecule”) or inactive state (represented by the presence of a  $D$  “molecule”). In the both states the protein  $A$  can be produced by the gene or degraded, but in the inactive state the production rate is assumed to be small. We will discuss exactly what the production rate means when we introduce the dynamic models. (In this model one does not explicitly keep track of the amount of mRNA, that is, the stages of transcription and translation are lumped together.) From a topological perspective, the reaction scheme is similar to (2.1) with  $B$  replaced by the empty set  $\emptyset$ :



The corresponding graph describes a CRN with three species  $\mathcal{S} = \{A, C, D\}$ . The set of complexes is now

$$\mathcal{C}_1 = C + A, \quad \mathcal{C}_2 = C, \quad \mathcal{C}_3 = D, \quad \mathcal{C}_4 = D + A,$$

such that



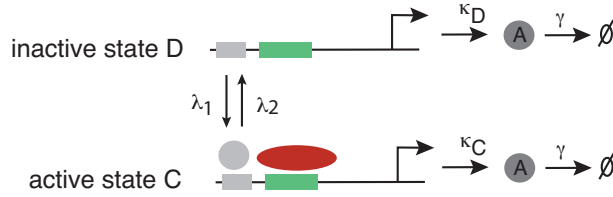


FIG. 2.2. Two-state gene regulatory network in which the promoter transitions between an active state  $C$  and inactive state  $D$  at rates  $\lambda_{1,2}$ . The corresponding production rates of protein  $A$  are  $\kappa_C, \kappa_D$ , respectively, and the protein degradation rate is  $\gamma$ . The terms active and inactive refer to the fact that  $\kappa_C > \kappa_D$ .

Hence, the stoichiometric matrix is

$$\mathbf{K} = \begin{bmatrix} -1 & 1 & 1 & -1 & 0 & 0 \\ 0 & 0 & 0 & 0 & -1 & 1 \\ 0 & 0 & 0 & 0 & 1 & -1 \end{bmatrix},$$

and the incidence matrix is

$$\mathbf{J} = \begin{bmatrix} -1 & +1 & 0 & 0 & 0 & 0 \\ +1 & -1 & 0 & 0 & -1 & 1 \\ 0 & 0 & -1 & +1 & 1 & -1 \\ 0 & 0 & +1 & -1 & 0 & 0 \end{bmatrix}.$$

It follows that the network has deficiency  $\delta = 1$ .

**2.2. Dynamic models in the classical setting.** In the previous subsection we introduced a purely topological description of a CRN. The subject of the present section is when the reactions occur. In the classical theory there are two models one considers—stochastic models in which reaction occur at exponentially distributed rates and deterministic models in which reactions occur continuously. While more difficult to study, the stochastic model, which includes the random effects of having a finite number of molecules in the system, is more accurate. The deterministic model is technically an approximation, neglecting the fine grained structure of the dynamics.

**2.2.1. Stochastic dynamics.** Let  $X_i(t)$  denote the number of molecules in the  $i$ th species at time  $t$  so that  $\mathbf{X}(t) = (X_1(t), \dots, X_m(t))^T$  describes the state of the system. Since the only changes in  $\mathbf{X}(t)$  are of the form  $\mathbf{X}(t) + \mathbf{K}_j$ , the evolution is confined to the set

$$\mathcal{Z}_{\mathbf{x}_0} = (\text{span}(\mathbf{K}) + \mathbf{x}_0) \cap \mathbb{N}^m.$$

In CRN theory the sets  $\mathcal{Z}_{\mathbf{x}_0}$  are known as *stoichiometric subspaces*. Assuming the *law of mass action*, the  $j$ th reaction occurs at exponentially distributed times with state dependent rate parameter [2]

$$(2.6) \quad \alpha_j(\mathbf{X}(t)) = \frac{\kappa_j}{\Omega^{\sum_i K_{j,i}^R - 1}} \prod_i \frac{X_i(t)!}{(X_i(t) - K_{j,i})!}.$$

The positive number  $\kappa_j$  is known as a *rate constant* associated with the reaction, while  $\Omega$  is a dimensionless parameter called the *system-size*. The combinatorial term

inside the product takes into account the fact the probability that  $r$  molecules of the same species are within a reaction radius is proportional to  $X_i(X_i - 1) \dots (X_i - r + 1)$ , which tends to  $X_i^r$  in the large  $\Omega$  limit. If  $X_i(t) = O(\Omega)$  for each species, then we say that the model is *classically scaled* and the factor  $\Omega^{-\sum_i K_{j,i}^R + 1}$  ensures

$$\alpha_j(\mathbf{X}(t)) = \Omega \alpha_j(\mathbf{X}(t)/\Omega) = O(\Omega).$$

That is, for a classically scaled model all reaction rates are roughly the same order of magnitude and grow monotonically with the system-size. This fact is crucial, as it allows us to derive the deterministic approximation presented below.

While there are many ways to describe the dynamics of  $\mathbf{X}(t)$ , we will present a representation based on the evolution of the probability distribution  $p(\mathbf{x}, t) = \mathbb{P}(\mathbf{X}(t) = \mathbf{x} | \mathbf{X}(0) = \mathbf{x}_0)$ . This is given by the *chemical master equation*

$$(2.7) \quad \frac{d}{dt} p(\mathbf{x}, t) = M p(\mathbf{x}, t) \quad p(\mathbf{x}, 0) = \mathbf{1}_{\{\mathbf{x}=\mathbf{x}_0\}},$$

where  $M$  is the linear operator

$$M f(\mathbf{x}) = \sum_j \alpha_j(\mathbf{x} - \mathbf{K}_j) f(\mathbf{x} - \mathbf{K}_j) - \alpha_j(\mathbf{x}) f(\mathbf{x}).$$

For a rigorous derivation of this form, including specific function space on which  $f(\mathbf{x})$  is defined, see [12]. We will assume the process  $\mathbf{X}(t)$  is ergodic, that is, we assume there exists a probability distribution  $\pi(\mathbf{x})$  satisfying  $\pi(\mathbf{x}) = \lim_{t \rightarrow \infty} p(\mathbf{x}, t)$ . While the computation of  $\pi$  is generally a hopeless task, it has been shown that for reversible, deficiency zero networks  $\pi(\mathbf{x})$  is given by a multivariate Poisson distribution [1].

**2.2.2. Reaction rate equations.** Historically, there has been a great deal of interest in understanding the behavior of the process  $\mathbf{X}(t)$  as  $\Omega$  becomes large [12]. Among other developments, this has led to a law of large numbers for the rescaled variables  $\mathbf{Z}(t) = \mathbf{X}(t)/\Omega$ . This was proved by Kurtz in [24] and says that  $\mathbf{Z}(t) \rightarrow \bar{\mathbf{z}}(t)$  almost surely, where  $\bar{\mathbf{z}}(t)$  satisfies the *reaction rate equations*

$$(2.8) \quad \frac{d}{dt} \bar{\mathbf{z}}(t) = \sum_{j=1}^p \bar{\alpha}_j(\bar{\mathbf{z}}(t)) \mathbf{K}_j, \quad \bar{\mathbf{z}}(0) = \mathbf{x}_0/\Omega.$$

Here the rate function  $\bar{\alpha}_j$  is obtained by taking the leading order term of (2.6) in  $\Omega^{-1}$ :

$$\bar{\alpha}_j(\bar{\mathbf{z}}(t)) = \kappa_j \prod_{i=1}^m \bar{z}_i(t)^{K_{j,i}^R}.$$

It's worth noting that this result can be derived heuristically by carrying out a system-size expansion; see [32]. The highly nonlinear nature of (2.8) makes understanding the behavior of these equations over long periods of time a challenging task. It turns out that when the deficiency is zero the existence of a stable equilibria within each  $\mathcal{Z}_{\mathbf{x}}$  is guaranteed, the intuition being that the dynamics can be understood by transforming the problem into a linear one on complex space. The precise statement of this result is the original deficiency zero theorem [13]. The proof makes use of the fact that

$$(2.9) \quad V(\mathbf{z}) = \sum_{i=1}^m z_i (\ln(z_i) - \ln(\zeta_i) - 1) + \zeta_i$$

is a Lyapunov function for (2.8) at the equilibria  $\zeta$ . When the deficiency of the underlying network is zero,  $V(\mathbf{z})$  is a strict Lyapunov function:  $\nabla V(\mathbf{z}) \leq 0$  with equality if and only if  $\mathbf{z} = \zeta$ .

**3. Examples of multiscale dynamics.** The assumption that all species in the system are roughly of equal abundance breaks down in many biochemical systems of interest. This has motivated the development of multiscale approximations where only a fraction of the species are taken to evolve continuously [10, 8, 27]. Below we present two examples of multiscale networks with very different behavior, while a more general derivation of the multiscale approximation is provided in section 4.

**Example 1.** As our first example, we revisit network (2.1) and compare three different dynamic models. For the stochastic model the right-hand side of the master equation is obtained by applying the operator

$$\begin{aligned} Mf(\mathbf{x}) = & \kappa_1(x_A + 1)x_C f\left(\begin{bmatrix} x_A + 1 \\ x_B - 1 \\ x_C \\ x_D \end{bmatrix}\right) + \kappa_2(x_B + 1)x_C f\left(\begin{bmatrix} x_A - 1 \\ x_B + 1 \\ x_C \\ x_D \end{bmatrix}\right) \\ & + \kappa_3(x_A + 1)x_D f\left(\begin{bmatrix} x_A + 1 \\ x_B - 1 \\ x_C \\ x_D \end{bmatrix}\right) + \kappa_4(x_B + 1)x_D f\left(\begin{bmatrix} x_A - 1 \\ x_B + 1 \\ x_C \\ x_D \end{bmatrix}\right) \\ & + \kappa_5 x_C f\left(\begin{bmatrix} x_A \\ x_B \\ x_C - 1 \\ x_D + 1 \end{bmatrix}\right) + \kappa_6 x_D f\left(\begin{bmatrix} x_A \\ x_B \\ x_C + 1 \\ x_D - 1 \end{bmatrix}\right) \\ & - (\kappa_1 x_A x_C + \kappa_2 x_B x_C + \kappa_3 x_A x_D + \kappa_4 x_B x_D + \kappa_5 x_C + \kappa_6 x_D) f(\mathbf{x}). \end{aligned}$$

Here  $\kappa_j$  is the reaction rate of the  $j$ th reaction with  $j = 1, \dots, 6$ . The computation of  $\pi$  satisfying  $M\pi(\mathbf{x}) = 0$  turns out to be exceedingly complicated, and as a result, one might turn to a deterministic approximation for insight. Taking the limit  $\Omega \rightarrow \infty$  we obtain the equations

$$\begin{aligned} \frac{d}{dt} z_A &= z_C(\kappa_2 z_B - \kappa_1 z_A) - z_D(\kappa_3 z_A - \kappa_4 z_B), \\ \frac{d}{dt} z_B &= z_D(\kappa_3 z_A - \kappa_4 z_B) - z_C(\kappa_2 z_B - \kappa_1 z_A), \\ \frac{d}{dt} z_C &= \kappa_6 z_D - \kappa_5 z_C, \\ \frac{d}{dt} z_D &= \kappa_5 z_C - \kappa_6 z_D. \end{aligned}$$

These equations can readily be solved in equilibria to obtain a unique steady state which is asymptotically stable. However, studying the reaction rate equation is problematic if the abundances vary over many orders of magnitude. For example, suppose  $X_A(t) + X_B(t) = O(\Omega)$  but there is initially only one  $D$  molecule and no  $C$  molecules. This type of scaling is typical of systems with extrinsic noise, which in the present context is represented by the switching between  $(X_C(t), X_D(t)) = (0, 1)$  and  $(X_C(t), X_D(t)) = (1, 0)$ . This is in contrast to the intrinsic, or demographic, noise, resulting from the finite values of  $X_A(t)$  and  $X_B(t)$ . If  $\Omega \gg 1$ , then between occurrences

of the 5th and 6th reactions the dynamics are well approximated by the reaction rate equations for  $z_A$  and  $z_B$ . On the other hand, if we attempt to model the system using the full set of reaction rate equations, information about the stochasticity resulting from the binary nature of  $X_D$  and  $X_C$  would be lost. This motivates a *multiscale reduction* in which only a fraction of the species are modeled as continuous variables.

In the present context, we would allow  $X_C(t)$  and  $X_D(t)$  to evolve according to their stochastic dynamics, while approximating the high copy species by

$$(3.1) \quad \begin{aligned} \frac{d}{dt} \bar{Z}_A(t) &= X_C(t)(\kappa_2 \bar{Z}_B(t) - \kappa_1 \bar{Z}_A(t)) - X_D(t)(\kappa_3 \bar{Z}_A(t) - \kappa_4 \bar{Z}_B(t)), \\ \frac{d}{dt} \bar{Z}_B(t) &= X_D(t)(\kappa_3 \bar{Z}_A(t) - \kappa_4 \bar{Z}_B(t)) - X_C(t)(\kappa_2 \bar{Z}_B(t) - \kappa_1 \bar{Z}_A(t)). \end{aligned}$$

The derivatives in this system are well defined between discontinuities of  $X_C(t)$  and  $X_D(t)$  corresponding to the firing of the 5th and 6th reactions. It can be shown that these reactions fire at times  $\tau_1, \tau_2, \dots$  satisfying

$$\mathbb{P}(\tau_{k+1} - \tau_k > T | X_C(\tau_k) = x) = e^{-T(x\kappa_5 + (1-x)\kappa_6)}.$$

The Markov process  $(\bar{Z}_A(t), \bar{Z}_B(t), X_C(t), X_D(t))$  is an example of a *piecewise deterministic Markov process* (PDMP). In Figure 3.1 we have displayed sample paths of this PDMP. Notice how the behavior of the multiscale network contrasts with the rather dull behavior of the deterministic dynamics, which we know converge to a stable equilibria over long periods of time. The network (2.1) shows that for multiscale systems a type of oscillatory behavior may be observed that is driven by noise, rather than dynamics.

Intuition about this phenomenon can also be gained by examining the equilibria of (3.1) for fixed values of  $X_C(t)$  and  $X_D(t)$ . Setting  $d\bar{Z}_A(t)/dt = 0$  in (3.1) and using the fact that  $\bar{Z}_B = 1 - \bar{Z}_A$  and  $X_D = 1 - X_C$ , we find that at equilibrium

$$X_A \equiv \zeta_A(X_C, X_D) = \frac{\kappa_2 X_C + \kappa_4 (1 - X_C)}{(\kappa_1 + \kappa_2) X_C + (\kappa_3 + \kappa_4) (1 - X_C)}.$$

Moreover, it can easily be checked that for all values of  $X_C$  this equilibria is stable. Therefore, in between jumps  $\bar{Z}_A$  will approach  $\zeta_A(X_C, X_D)$ . When a jump occurs,

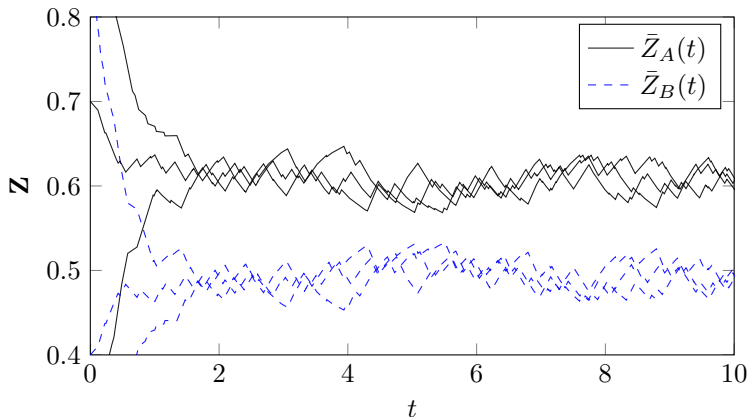


FIG. 3.1. Realization of the PDMP corresponding to (2.1) with  $\kappa_1 = \kappa_3 = \kappa_4 = 1$ ,  $\kappa_2 = 1.5$ , and  $\kappa_5 = \kappa_6 = 10$ .

$\zeta_A(X_C, X_D)$  moves to  $\zeta_A(X_C + 1, X_D - 1)$  or  $\zeta_A(X_C - 1, X_D + 1)$  and the system begins to approach this new equilibria. After a long period of time  $\bar{Z}_A(t)$  will become trapped between all possible values of  $\zeta_A(X_C, X_D)$ . This is exactly what we observed in Figure 3.1. One final point is that if  $\kappa_2 = \kappa_4$  and  $\kappa_1 = \kappa_3$ , then  $\zeta_A$  becomes independent of  $X_C$  and  $X_D$ , resulting in deterministic behavior for  $t \rightarrow \infty$ . However, this only occurs for nongeneric choices of the reaction rates, in contrast to the next example.

**Example 2.** We now present an example of a network that appears similar in structure to (2.1), but has dramatically different behavior in the multiscale setting. The network of interest is



The only modification that has been made from the previous example is the replacement of  $B$  with  $2A$  in reactions 3 and 4. In terms of the complexes this means replacing  $\mathcal{C}_4$  in the previous example with  $\mathcal{C}_4 = 2A + D$ . The graph on complex space shown in (2.2) is invariant with respect to this modification, and therefore  $\ker(\mathbf{J})$  remains unchanged. On the other hand, the stoichiometric matrix corresponding to (3.2) is

$$\mathbf{K} = \begin{bmatrix} -1 & 1 & 1 & -1 & 0 & 0 \\ 1 & -1 & 0 & 0 & 0 & 0 \\ 0 & 0 & 0 & 0 & -1 & 1 \\ 0 & 0 & 0 & 0 & 1 & -1 \end{bmatrix}.$$

This matrix has a three-dimensional nullspace, from which we can compute  $\delta = 0$ . In summary, going from (2.1) to (3.2) has the effect of changing the deficiency from 1 to 0. As a consequence we know that the latter stochastic model has a unique Poisson like stationary density, and the corresponding deterministic version of the model converges to a stable equilibria for suitable initial conditions. As we will see, this has a significant impact on the multiscale dynamics.

Suppose once again that species  $A$  and  $B$  are in high copy, while  $C$  and  $D$  are in low copy. The continuous dynamics are then given by the PDMP

$$\begin{aligned} \frac{d}{dt} \bar{Z}_A &= X_C(\kappa_2 \bar{Z}_B - \kappa_1 \bar{Z}_A) + X_D \bar{Z}_A(\kappa_4 \bar{Z}_A - \kappa_3), \\ \frac{d}{dt} \bar{Z}_B &= X_C(\kappa_1 \bar{Z}_A - \kappa_2 \bar{Z}_B). \end{aligned}$$

The sample paths of the PDMP modeling (3.2) are displayed in Figure 3.2. In contrast to the previous example, we see that while the continuous components of the dynamics initially evolve stochastically, they appear to become coherent after a long period of time. To explain this phenomenon, we look at the equilibria of the continuous dynamics,

$$\zeta_A = \frac{\kappa_3}{\kappa_4} \quad \zeta_B = \frac{\kappa_1 \kappa_3}{\kappa_2 \kappa_4}.$$

The key fact to note is that  $X_C$  does not appear in these expressions, suggesting that the extrinsic noise has no effect on the behavior over long periods of time. In the next section we will show that this is related to the network deficiency. It is important to

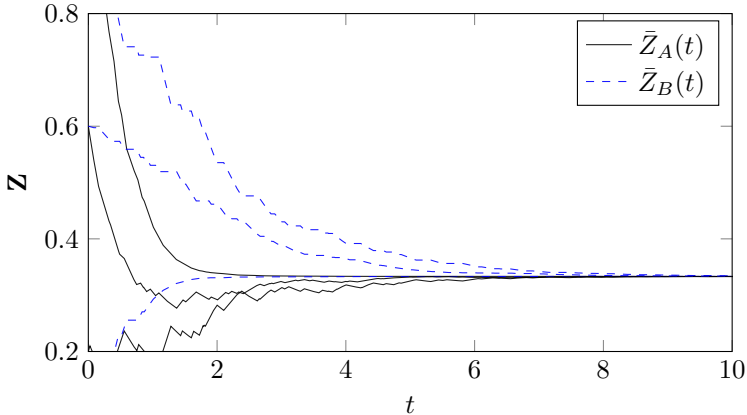


FIG. 3.2. Realizations of the PDMP corresponding to (3.2) with different initial conditions and  $\kappa_1 = \kappa_3 = 1$ ,  $\kappa_4 = \kappa_2 = 0.8$ , and  $\kappa_5 = \kappa_6 = 10$ . It can be seen that although the system is initially stochastic, given enough time  $Z_A(t)$  and  $Z_B(t)$  tend toward a deterministic value.

remark that this behavior indicates that the stationary density of the continuous time Markov chain model becomes singular in the thermodynamic limit, and as such, one cannot directly use the master equation formulation to obtain rigorous results.

#### 4. Robustness and deficiency.

**4.1. The multiscale reduction.** In order to present our general results, we formalize the multiscale reduction performed on the networks (2.1) and (3.2). Similar procedures can be found in many other studies [8, 21]. The first step is to decompose  $\mathcal{S}$  by writing  $\mathcal{S} = (\mathcal{S}^{(1)}, \mathcal{S}^{(2)})$  with  $\mathcal{S}^{(1)} = (\mathcal{S}_1, \dots, \mathcal{S}_{m_1})$  and  $\mathcal{S}^{(2)} = (\mathcal{S}_{m_1+1}, \dots, \mathcal{S}_{m_1+m_2})$  representing the high and low copy species, respectively. For  $\mathcal{S}_i \in \mathcal{S}^{(1)}$ , we assume  $X_i(t) = O(\Omega)$ , where  $\Omega$  is again the system size. In other words, the species in  $\mathcal{S}^{(1)}$  are in high copy, while those in  $\mathcal{S}^{(2)}$  are in low copy. The next step is to impose some constraints on the network structure that force the initial copy numbers to be preserved in time. This is done by observing that in a multiscale network each reaction can be written in the form

$$\sum_{i=1}^{m_1} U_{j,i}^R \mathcal{S}_i + \sum_{i=m_1+1}^{m_1+m_2} V_{j,i}^R \mathcal{S}_i \longrightarrow \sum_{i=1}^{m_1} U_{j,i}^P \mathcal{S}_i + \sum_{i=m_1+1}^{m_1+m_2} V_{j,i}^P \mathcal{S}_i.$$

We have decomposed the reaction directions according to  $\mathbf{K} = (\mathbf{U}, \mathbf{V})$  with  $\mathbf{U}_j = \mathbf{U}_j^P - \mathbf{U}_j^R$  and  $\mathbf{V}_j = \mathbf{V}_j^P - \mathbf{V}_j^R$ . The form of these reactions played a particularly important role in the examples above, namely, each reaction changed either high or low copy species, but not both. Intuitively, it makes sense that in a multiscale system the different scales should evolve orthogonally; otherwise there is a possibility that a high copy species produces a low copy species, disrupting the separation of scales. While it is possible to account for reactions that change both high and low copy species using more sophisticated scalings [22], we will exclude such cases from our analysis and adopt the following assumption.

**ASSUMPTION 1.** *A multiscale CRN satisfies the following orthogonality property: either  $\mathbf{U}_j = \mathbf{0}$  or  $\mathbf{V}_j = \mathbf{0}$  for each  $j = 1, \dots, p$ .*

We will also order the reactions such that  $\mathbf{U}_j = \mathbf{0}$  when  $j = 1, \dots, p_1$  and  $\mathbf{V}_j = \mathbf{0}$

when  $j = p_1 + 1, \dots, p_1 + p_2 = p$ . In order to represent the evolution of the process, we decompose the state variable into the high and low copy components by setting  $\mathbf{X} = (\mathbf{X}^{(1)}, \mathbf{X}^{(2)})$ . The  $m_2$  dimensional vector  $\mathbf{X}^{(2)}$  is related to  $\mathbf{X}$  by  $X_i^{(2)}(t) = X_{m_1+i}(t)$ . Our objective is to approximate the process  $\mathbf{X}$  with a process  $\bar{\mathbf{X}}$  obtained in the limit  $\Omega \rightarrow \infty$ . It is assumed that reactions changing  $\mathcal{S}^{(1)}$  species are  $O(\Omega)$ , while reactions changing  $\mathcal{S}^{(2)}$  species are  $O(1)$ . Such a separation of timescales can be achieved by rescaling the constant factor in (2.6) according to

$$\kappa_j \Omega^{-\sum_{i=1}^{m_1} U_{j,i+1}} \rightarrow \kappa_j \Omega^{-\sum_{i=1}^{m_1} U_{j,i}}$$

if  $j > p_1$ . This ensures  $\alpha_j(\mathbf{x}^{(1)}, \mathbf{x}^{(2)}) = O(1)$  for the reactions changing low copy species. At this point it is useful to introduce the scaled variables  $\mathbf{Z}_i = \mathbf{X}_i/\Omega$ . Since  $\mathbf{Z}_i = O(1)$ , these process are easier to work with in the large system-size limit. In particular, the multiscale process (2.7) becomes

$$(4.1) \quad \frac{d}{dt} p(\mathbf{z}^{(1)}, \mathbf{x}^{(2)}, t) = M_1 p(\mathbf{z}^{(1)}, \mathbf{x}^{(2)}, t) + M_2 p(\mathbf{z}^{(1)}, \mathbf{x}^{(2)}, t),$$

where

$$\begin{aligned} M_1 f(\mathbf{z}^{(1)}, \mathbf{x}^{(2)}) &= \Omega \sum_{j=1}^{p_1} \alpha_j(\mathbf{z}^{(1)} - \mathbf{U}_j/\Omega, \mathbf{x}^{(2)} - \mathbf{V}_j) f(\mathbf{z}^{(1)} - \mathbf{U}_j/\Omega, \mathbf{x}^{(2)} - \mathbf{V}_j) \\ &\quad - \alpha_j(\mathbf{z}^{(1)}, \mathbf{x}^{(2)}) f(\mathbf{z}^{(1)}, \mathbf{x}^{(2)}), \\ M_2 f(\mathbf{z}^{(1)}, \mathbf{x}^{(2)}) &= \sum_{j=p_1+1}^{p_2} \alpha_j(\mathbf{z}^{(1)} - \mathbf{U}_j/\Omega, \mathbf{x}^{(2)} - \mathbf{V}_j) f(\mathbf{z}^{(1)} - \mathbf{U}_j/\Omega, \mathbf{x}^{(2)} - \mathbf{V}_j) \\ &\quad - \alpha_j(\mathbf{z}^{(1)}, \mathbf{x}^{(2)}) f(\mathbf{z}^{(1)}, \mathbf{x}^{(2)}). \end{aligned}$$

In the limit  $\Omega \rightarrow \infty$ , it can be shown that  $\mathbf{Z}^{(1)}(t) \rightarrow \bar{\mathbf{Z}}^{(1)}(t)$ , where  $\bar{\mathbf{Z}}^{(1)}(t)$  is given by the PDMP [27]

$$(4.2) \quad \frac{d}{dt} \bar{\mathbf{Z}}^{(1)}(t) = \sum_{j=1}^{p_1} \bar{\alpha}_j(\bar{\mathbf{Z}}^{(1)}(t), \mathbf{X}^{(2)}(t)) \mathbf{U}_j$$

The state-space of  $\bar{\mathbf{Z}}^{(1)}(t)$  with  $\bar{\mathbf{Z}}^{(1)}(0) = \mathbf{z}_0$  is some subset of

$$\bar{\mathcal{Z}}_{\mathbf{z}_0} = (\text{span}(\mathbf{K}) + \mathbf{z}_0) \cap \mathbb{R}_{\geq 0}^m.$$

In contrast to (2.8), these equations now involve  $\bar{\mathbf{X}}^{(2)}(t)$  which evolves according to a Markov jump process generated by  $\bar{M}_2(\mathbf{Z}^{(1)}(t))f(\mathbf{x}^{(2)}) = M_2 f(\mathbf{Z}^{(1)}(t), \mathbf{x}^{(2)})$ . Note that if  $\mathcal{S}^{(2)} = \emptyset$ , we retrieve the reaction rate equations (2.8).

**4.2. Result for deficiency zero systems.** We now direct our attention toward the network deficiency and its relationship to the multiscale dynamics. Our main result is summarized in the following theorem, which explains the behaviors observed in section 3.

**THEOREM 4.1.** *Suppose  $\bar{\mathbf{Z}}^{(1)}(t)$  evolves according to the PDMP model of a deficiency zero and reversible CRN satisfying Assumption 1. Then there exists a deterministic fixed point  $\zeta$  of the process (4.2). Moreover,  $\mathbf{Z}^{(1)}(t) \rightarrow \zeta$  almost surely when  $\mathbf{Z}^{(1)}(0)$  is sufficiently close to  $\zeta$ .*

The implication of this result is that networks satisfying the assumption of Theorem 4.1 are robust to extrinsic noise, i.e., noise due to environmental changes or random external inputs. This is particularly relevant when considering a population of CRNs, as we will in section 5.

*Proof.* For simplicity, assume that  $\|\mathbf{V}_j^R\|_1 = \|\mathbf{V}_j^P\|_1 = 1$  for  $j = 1, \dots, p_1$ . That is, each reaction changing the high copy species is catalyzed by exactly one low copy species. The argument below can easily be applied to the more general setting with some minor modifications of the notation. A key observation is that Assumption 1 allows us to write (4.2) in the form

$$(4.3) \quad \frac{d\bar{\mathbf{Z}}^{(1)}(t)}{dt} = \sum_{i=1}^{m_2} X_i^{(2)}(t) \mathbf{H}_i(\bar{\mathbf{Z}}^{(1)}(t)),$$

where  $\mathbf{H}_s(\mathbf{z})$  represents the dynamics associated with the linkage class catalyzed by  $X_s^{(2)}$ .<sup>2</sup> For example, in the network (3.2), the dynamics catalyzed by  $X_C(t)$  are

$$\mathbf{H}_1(\bar{z}_A, \bar{z}_B) = \begin{bmatrix} \kappa_2 \bar{z}_B - \kappa_1 \bar{z}_A \\ -\kappa_2 \bar{z}_B + \kappa_1 \bar{z}_A \end{bmatrix}.$$

Since the deficiency of the network is zero, any closed cycles of reaction vectors are realized by reactions confined to one of these linkage classes. The continuous dynamics of (4.2) admit a deterministic fixed point provided there exists a solution to the equations

$$(4.4) \quad \mathbf{H}_i(\boldsymbol{\zeta}) = 0, \quad i = 1, \dots, m_2.$$

We will establish the existence of such a fixed point first, and then discuss the stability.

Suppose that the reactions are ordered such that

$$\mathbf{H}_s(\mathbf{z}) = \sum_{j=l_{s-1}+1}^{l_s} \left( \kappa_j \prod_{i=1}^{m_1} z_i^{K_{j,i}^R} \right) \mathbf{U}_j.$$

That is, there are  $l_s$  reactions corresponding to the linkage class  $s$ , which are all catalyzed by  $X_s^{(2)}$ . Then

$$\mathcal{H}_i = \text{span}\{\mathbf{U}_{l_{i-1}+1}, \mathbf{U}_{l_{i-1}+2}, \dots, \mathbf{U}_{l_i}\}$$

represents the reachable states in  $\mathbb{R}^{m_1}$  through reactions catalyzed by the  $i$ th species, modulo the addition of a constant vector. Each  $\mathbf{H}_s(\mathbf{z})$  can be associated with a CRN involving only the reactions in the corresponding linkage class. Since removing linkage classes can only decrease the number of cycles that are not realized in the reaction graph, the deficiency of the CRN associated with any linkage class of a deficiency zero network must also be zero. It is therefore a consequence of the deficiency zero theorem that the equations  $\mathbf{H}_i(\boldsymbol{\zeta}) = 0$  have independent solutions.<sup>3</sup>

Without loss of generality, suppose the solution to  $\mathbf{H}_1(\boldsymbol{\zeta}) = 0$  is unique and depends only on the components  $\zeta_1, \zeta_2, \dots, \zeta_k$ . Within the linkage class corresponding to  $\mathbf{H}_1$ , each of the species  $\mathcal{S}_1, \mathcal{S}_2, \dots, \mathcal{S}_k$  must be both produced and degraded. To see

<sup>2</sup>Each connected component of a CRN is called a linkage class.

<sup>3</sup>Recall that the deficiency zero theorem states that a reversible, deficiency zero network has an equilibria in  $\bar{\mathcal{Z}}_{\mathbf{z}_0}$  for each  $\mathbf{z}_0$  [14].

this, note that if a species is unchanged by reactions within a linkage class any terms in  $\mathbf{H}_1$  involving that species can be factored out of the entire expression for  $\mathbf{H}_1(\zeta)$ , which contradicts the assumption that the roots of these expression depend on the first  $k$  species. Moreover, since the solution is assumed to be unique in these species, no quantity is conserved by these reactions; otherwise there would be an extra degree of freedom. It follows that  $k$  of the vectors in  $\mathbf{U}_1, \dots, \mathbf{U}_{l_1}$  are linearly independent, and in particular,

$$\mathcal{H}_1 = \text{span}\{\mathbf{e}_1, \mathbf{e}_2, \dots, \mathbf{e}_k\},$$

where  $\mathbf{e}_k$  are basis vectors of the appropriate dimension.

Now suppose that the first two equations in (4.4) cannot be solved simultaneously. This implies that

$$\mathcal{H}_2 \cap \mathcal{H}_1 = \text{span}\{\mathbf{e}_1, \dots, \mathbf{e}_r\}$$

for some  $1 < r \leq k$ . In other words,  $\mathcal{H}_2 \cap \mathcal{H}_1$  is not empty or a single point. Using this fact, a cycle of reactions that is not realized in the graph on complex space can be constructed, contradicting the assumption that the network is deficiency zero. The construction begins by selecting distinct points  $\mathbf{z}_0, \mathbf{z}_1 \in \mathcal{H}_2 \cap \mathcal{H}_1$ . This allows one to write  $\mathbf{z}_1 = \mathbf{z}_0 + \sum_j \mathbf{U}_j$ , where the sum is taken over elements of  $\{1, \dots, l_1\}$  or  $\{l_1 + 1, \dots, l_2\}$ . That is,  $\mathbf{z}_1$  can be reached from  $\mathbf{z}_0$  using reactions from the linkage class catalyzed by  $\mathcal{S}_1^{(2)}$  or  $\mathcal{S}_2^{(2)}$ . Similarly, let  $\mathbf{x}_0 \in \mathbb{N}^{m_2}$  and  $\mathbf{x}_1 = \mathbf{x}_0 + \sum_j \mathbf{V}_j$  be accessible from  $\mathbf{x}_0$  by low copy reactions. Now a cycle in  $\mathbb{R}^{m_1} \times \mathbb{N}^{m_2}$  of the form

$$(\mathbf{z}_0, \mathbf{x}_0), \dots, (\mathbf{z}_1, \mathbf{x}_0), \dots, (\mathbf{z}_1, \mathbf{x}_1), \dots, (\mathbf{z}_0, \mathbf{x}_1), \dots, (\mathbf{z}_0, \mathbf{x}_0) \in \mathbb{R}^{m_1} \times \mathbb{N}^{m_2}$$

is given by taking reactions corresponding to  $\mathbf{H}_1$  from  $\mathbf{z}_0$  to  $\mathbf{z}_1$ , taking low copy reactions from  $\mathbf{x}_0$  to  $\mathbf{x}_1$ , and reactions corresponding to  $\mathbf{H}_2$  from  $\mathbf{z}_1$  to  $\mathbf{z}_0$ . The reversibility of the network guarantees the existence of a path from  $\mathbf{x}_0$  to  $\mathbf{x}_1$  and back again. This construction is illustrated for (2.1) in Figure 4.1, which is essentially Figure 2.1 redrawn using the notation of this proof. In Figure 4.2 we show why the construction of such a cycle cannot be performed for the deficiency zero network (3.2). At this point we deduce that for a deficiency zero network, the equations  $\mathbf{H}_1(\zeta) = 0$  and  $\mathbf{H}_2(\zeta) = 0$  can be solved simultaneously. The construction of such a cycle can also be performed if the solution to  $\mathbf{H}_i(\zeta) = 0$  is not compatible with the solutions to  $\mathbf{H}_s(\zeta) = 0$  with  $s = 1, \dots, i-1$ . It follows that (4.4) has a solution in any network satisfying the hypothesis of the theorem.

In order to establish that the solution is attracting and unique within  $\bar{\mathcal{Z}}_{\mathbf{z}_0}$ , we make use of the deficiency zero theorem. Removing the reactions indexed by  $p_1$  through  $p_1 + p_2$  does not change the deficiency of the network. As a consequence, (4.3) has a unique solution that is stable for each value of  $\mathbf{X}^{(2)}$ . As we have shown, this solution  $\zeta$  is independent of the low copy dynamics. In order to establish that  $\zeta$  is an almost sure limit of  $\mathbf{Z}^{(1)}(t)$  we can utilize [7, Theorem 3.1]. This results states that almost sure convergence will occur provided there exists a function  $V(\mathbf{z})$  which is a strict Lyapunov function for (4.3) and is independent of  $X_i^{(2)}$ . This follows from the fact that (2.9) only depends on the reaction rate constants implicitly through  $\zeta$ .  $\square$

**4.3. Result for positive deficiency systems.** In light of Theorem 4.1, it is natural to ask when the PDMPs modeling networks with positive deficiency have nondeterministic behavior in the limit  $t \rightarrow \infty$ . Most of the work toward a solution

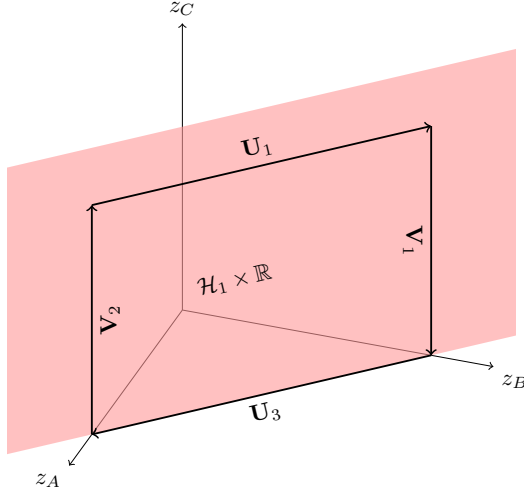


FIG. 4.1. A diagram of the construction in the proof of Theorem 4.1 for the network given in (2.1). In this case  $\mathcal{H}_1 = \mathcal{H}_2 = \{\mathbf{z} \in \mathbb{R}^2 : \mathbf{1}^T \mathbf{z} = 0\}$  so we can construct a cycle in state space that is not realized in the reaction graph. Of course, this forces the deficiency to be one, and therefore the network fails the hypothesis of the theorem.

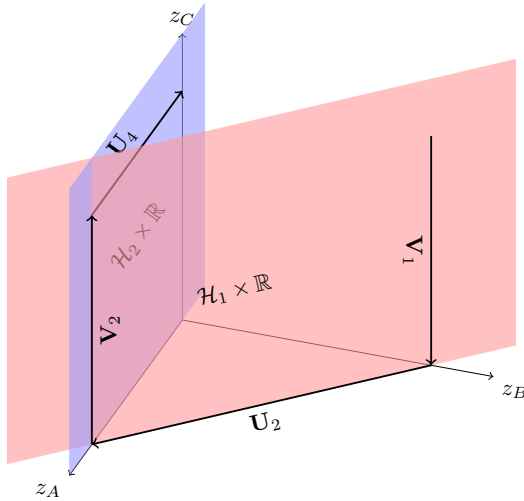


FIG. 4.2. An illustration of how the construction in the proof of Theorem 4.1 cannot be performed on (3.2). In this case  $\mathcal{H}_1 \cap \mathcal{H}_2 = \{(1, 0, 0)^T\}$ .

to this problem is actually contained in the proof of Theorem 4.1. What this proof suggests is that the vector valued functions  $\mathbf{H}_s(\mathbf{z})$  can potentially have incompatible roots when the sets  $\mathcal{H}_s$  intersect in the correct way. This was illustrated in Figure 4.1. For positive deficiency networks, we can force two sets  $\mathcal{H}_1$  and  $\mathcal{H}_2$  to intersect by creating a cycle that connects the linkage classes corresponding to these sets. This is the mathematical motivation for the following assumption.

ASSUMPTION 2. A multiscale CRN satisfies the following properties:

- (i) There are at least two linkage classes in the CRN, each involving reactions that

change high copy species. When considered as independent CRNs, these linkage classes are deficiency zero.

- (ii) There is a cycle, corresponding to some  $\mathbf{c} \in \ker(\mathbf{K})$ , that contains reactions in both linkage classes from (i).
- (iii) Both linkage classes from (i) are catalyzed by different low copy species.

From a physical perspective, Assumption 2 implies that different states of the low copy dynamics can push the system in different directions. This behavior was seen in the network (2.1). Indeed, it is easy to see that (2.1) satisfies Assumption 2: The two linkage classes referred to in part (i) are



and



the cycle of part (ii) corresponds to  $\mathbf{c} = (1, 0, 1, 0, 1, 1)^T$  and was depicted in Figure 2.1, and the linkage classes are clearly catalyzed by different species. By the same argument we see that the gene network (2.4) also satisfies Assumption 2. We now state our main result for positive deficiency networks.

**THEOREM 4.2.** *Suppose  $\bar{\mathbf{Z}}^{(1)}(t)$  evolves according to the PDMP model of a deficiency  $\delta > 0$  and reversible CRN satisfying Assumptions 1 and 2. Moreover, assume the process  $\mathbf{X}^{(1)}(t)$  is recurrent. Then there is a choice of rate constants  $\{\kappa_1, \dots, \kappa_p\}$  such that  $\bar{\mathbf{Z}}^{(1)}(t)$  does not have an almost sure limit as  $t \rightarrow \infty$  for any  $\bar{\mathbf{Z}}^{(1)}(0)$ .*

*Proof.* We once again assume  $\|\mathbf{V}_j^R\|_1 = \|\mathbf{V}_j^P\|_1 = 1$  for  $j = 1, \dots, p_1$  and note that the argument below can easily be applied to the more general setting with some minor modifications of the notation. Using the notation introduced in the proof of Theorem 4.1, let  $\mathcal{H}_1$  and  $\mathcal{H}_2$  be the spans of the reaction vectors  $\mathbf{U}_j$  corresponding to the linkage classes of Assumption 2(i). It is a consequence of Assumption 2(ii) and Assumption 1 that

$$c_1 \mathbf{U}_1 + \dots + c_{l_1} \mathbf{U}_{l_1} = -(c_{l_1+1} \mathbf{U}_{l_1+1} + \dots + c_{l_2} \mathbf{U}_{l_2}).$$

Here  $c_i$  are the entries of  $\mathbf{c}$  defined in Assumption 2(ii). This shows that

$$\mathcal{H}_1 \cap \mathcal{H}_2 = \text{span}\{\mathbf{e}_1, \dots, \mathbf{e}_r\}$$

for some  $r \geq 1$ . The existence of  $\zeta_s$  satisfying  $\mathbf{H}_s(\zeta_s) = 0$  for  $s = 1, 2$  follows from Assumption 2(i). So far we have shown there is potential for  $\zeta_1 \neq \zeta_2$  in components  $r = 1, \dots, r$ , but it remains to prove that the rate constants can be selected to ensure this. To do so, we arbitrarily assign the cycle  $\mathbf{c}$  to be in the forward direction. Therefore,  $-\mathbf{c}$  represents the backward direction. Now by selecting all the rate constants  $\kappa_1, \dots, \kappa_{l_1}$  to be relatively large in the forward direction, the solution  $\zeta_1$  will be forced toward some  $\zeta^+$  which points in the direction of the cycle:

$$\zeta^+ = \bar{\mathbf{Z}}^{(1)}(0) + w^+(c_1 \mathbf{U}_1 + \dots + c_{l_1} \mathbf{U}_{l_1})$$

for some  $w^+ > 0$ . Similarly, by selecting all the rate constants  $\kappa_{l_1+1}, \dots, \kappa_{l_2}$  to be

relatively large in the backward direction,  $\zeta_2$  will approach

$$\begin{aligned}\zeta^- &= \bar{\mathbf{Z}}^{(1)}(0) + w^-(c_{l_1+1}\mathbf{U}_{l_1+1} + \cdots + c_{l_2}\mathbf{U}_{l_2}) \\ &= \bar{\mathbf{Z}}^{(1)}(0) - w^-(c_1\mathbf{U}_1 + \cdots + c_{l_1}\mathbf{U}_{l_1})\end{aligned}$$

for some  $w^- > 0$ . Therefore,

$$\zeta^+ - \zeta^- = (w^+ + w^-)(c_1\mathbf{U}_1 + \cdots + c_{l_1}\mathbf{U}_{l_1}) \in \mathcal{H}_1 \cap \mathcal{H}_2,$$

which implies that for some possibly extreme values of the rate constants,  $\zeta_1$  and  $\zeta_2$  differ in components  $i = 1, 2, \dots, r$ . It follows that the dynamics of the PDMP (4.2) approach different fixed points depending on the realization of the low copy dynamics. The recurrence of  $\mathbf{X}^{(1)}(t)$  rules out the possibility of almost every realization resulting in the same fixed point, so the result follows.  $\square$

Note that because irreversible networks are obtained in the limit as reaction rates become small, Theorem 4.2 is true for irreversible networks provided all the irreversible reactions are going in the same direction along the cycles constructed in the proof above. (Equation (2.4) is an example of such a network.) It is also worth noting that Theorems 4.1 and 4.2 can be extended to systems with nonmass action kinetics by replacing the definition of  $\mathbf{H}_s(\mathbf{z})$  with

$$\mathbf{H}_s(\mathbf{z}) = \sum_{j=l_{s-1}+1}^{l_s} f_j(\mathbf{z})\mathbf{U}_j,$$

where  $f_j(\mathbf{z})$  encodes the reaction rate kinetics. In the proof of Theorem 4.1 we have used the fact that  $f_j(\mathbf{z})$  is given by mass-action kinetics to (I) establish that  $\mathbf{H}_s(\zeta) = 0$  has a unique and stable solution and (II) to establish that stochastic dynamics converge almost surely. Therefore, assuming that  $f_j$  are selected such that conditions (I) and (II) hold, one can obtain a version of Theorems 4.1 and 4.2 for systems with nonmass action kinetics. In future publications we hope to discuss the details of how these results are applied to systems with nonmass action kinetics in greater depth.

**5. Implications for population level correlations.** Thus far the selection of intrinsic and extrinsic noise has been somewhat arbitrary. There is nothing inherently extrinsic about the low copy dynamics in networks (2.1) and (3.2), for example. We now introduce a population level perspective where the low copy dynamics are explicitly extrinsic. A motivating example is a population of noninteracting cells, each containing the gene regulatory network of Figure 2.2, which is driven by a randomly switching environment [31, 4]. Whether or not each gene is active depends on the state of the environment, which will be common to all cells evolving in the same environment. The discrete environmental states could represent the presence of some extracellular metabolite or signaling molecule, perhaps arising from changes in the physiological or hormonal state that a cell experiences in a multicellular organism. Variations in the population of cells may cause small differences in the model parameters, but the topological structure of each reaction network within the population is assumed to be identical. While the chemical systems might not interact over a timescale that is relevant to the function they perform, they are correlated through the common environment in which they evolve. This interpretation leads to an entirely new set of interesting statistics, namely, those corresponding to the *population level* description [26, 5]. These statistics measure the degree to which environmental factors introduce correlations between individuals (cells or organisms) in a population.

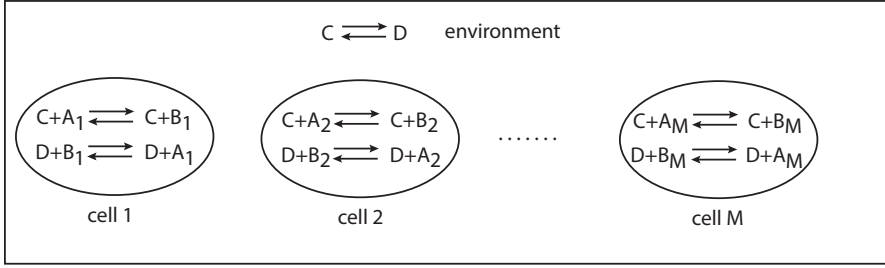


FIG. 5.1. A diagram of the CRN representing a population of CRNs in an environment.

Let us make the notion of population level statistics precise by returning to the network (3.2). As written in section 3, this is a single network whose dynamics exist in isolation. In the present setting we consider the reactions involving species  $A$  and  $B$  to be occurring in many cells inside common environment, while the reactions involving  $C$  and  $D$  are a property of this extracellular environment itself. If there are  $M$  cells in the environment, then the entire system, including the population and environment, can be written as a single CRN as indicated in Figure 5.1. We will let  $\kappa_{j,k}$  correspond to the rate constant of the  $j$ th reaction in the  $k$ th cell and allow for the possibility that  $\kappa_{j,k} \neq \kappa_{j,s}$  for  $s \neq k$ .

Building on the notation used in previous sections, we let  $X_{A_k}(t)$  denote the number of species  $A$  in cell  $k$ . It is not difficult to see that  $X_{A_k}(t)$  is equivalent in distribution to the variables  $X_A(t)$  used in section 3 if the appropriate rate constants are selected. What might be less clear is that the density

$$\mathbb{P}(X_{A_1}(t) = x_{A_1}, X_{A_1}(t) = x_{A_2}, \dots, X_{A_1}(t) = x_{A_M})$$

cannot be expressed in terms of the density of the single cell model in a trivial way. In particular, it is generally the case that

$$\mathbb{E}[X_{A_1}(t)X_{A_2}(t) \dots X_{A_k}(t)] \neq \prod_{k=1}^K \mathbb{E}[X_{A_k}(t)] \quad K \leq M.$$

It's important to emphasize that the correlations are induced by the environment and differences in the rate constants, but not the demographic noise. For this reason, we also have

$$\mathbb{E}[\bar{Z}_{A_1}(t)\bar{Z}_{A_2}(t) \dots \bar{Z}_{A_k}(t)] \neq \prod_{k=1}^K \mathbb{E}[\bar{Z}_{A_k}(t)] \quad K \leq M,$$

where  $\bar{Z}_{A_k}(t)$  is the PDMP approximation of  $X_{A_k}(t)$ . These new statistics, which do not appear in the single cell model, are what we refer to as a population level statistics, and it has been established that their computation is highly nontrivial, even for simple networks. Existing techniques for understanding such statistics involve taking the large population limit:  $M \rightarrow \infty$  [26]. In contrast, our results are applicable when it is appropriate to take the large system size limit  $\Omega \rightarrow \infty$ , while keeping  $M$  fixed. Implicit in our analysis is the assumption that  $\Omega$  is well defined at the population level.

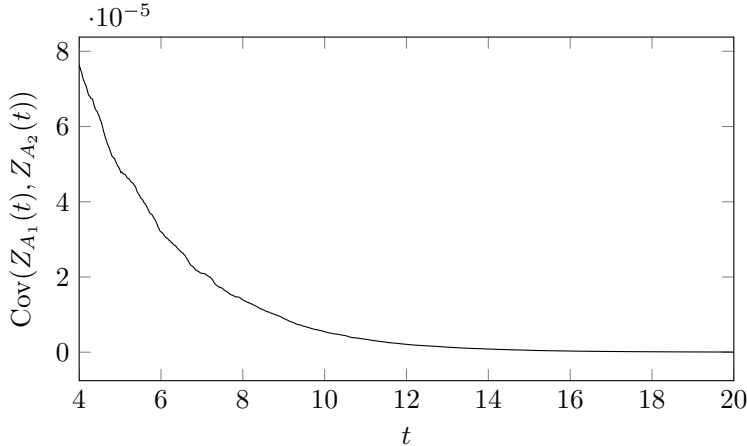


FIG. 5.2. The covariance for the population level model of (3.2) with  $M = 2$ ,  $\kappa_{1,1} = \kappa_{2,1} = \kappa_{3,1} = \kappa_{4,1} = 1$ ,  $\kappa_{1,2} = \kappa_{2,2} = 0.8$ ,  $\kappa_{3,2} = \kappa_{4,2} = 1.2$ , and  $\kappa_5 = \kappa_6 = 10$ .

In general, given a multiscale network satisfying Assumption 1 described in section 4, we can construct a population level model as follows. To avoid technicalities, we will assume  $\mathbf{X}^{(2)}(t)$  does not depend on  $\mathbf{X}_k^{(1)}(t)$ , although this assumption can easily be relaxed. Let  $\mathbf{X}_1^{(1)}(t), \mathbf{X}_2^{(1)}(t), \dots, \mathbf{X}_M^{(1)}(t)$  be identical copies of the random variable  $\mathbf{X}^{(1)}(t)$  constructed such that in between reactions indexed by  $j = p_1 + 1, \dots, p_1 + p_2$  each  $\mathbf{X}_k^{(1)}(t)$  evolve independently according to the same CRN, but with possibly different rate constants. When a transition in  $\mathbf{X}^{(2)}(t)$  does occur, it affects each  $\mathbf{X}_k^{(1)}(t)$  so that the sample paths of the high copy species are correlated through  $\mathbf{X}^{(2)}(t)$ . Theorem 4.1 then has the following implications for the population level statistics: if  $\bar{\mathbf{Z}}_k^{(1)} = \lim_{\Omega \rightarrow \infty} \mathbf{X}_k^{(1)}(t)/\Omega$  becomes deterministic, the correlations vanish. We state this observation as a corollary of Theorem 4.1.

COROLLARY 5.1. Let  $\bar{\mathbf{Z}}_1^{(1)}(t), \bar{\mathbf{Z}}_2^{(1)}(t), \dots, \bar{\mathbf{Z}}_M^{(1)}(t), \mathbf{X}^{(2)}(t)$  be a PDMP approximation of the population level model corresponding to a network satisfying the assumptions of Theorem 4.1. If  $\bar{\mathbf{Z}}_k^{(1)}(0)$  are sufficiently close to the equilibria  $\zeta$  for all  $k$ ,

$$\mathbb{E} \left[ \prod_{k=1}^K \bar{\mathbf{Z}}_k^{(1)}(t) \right] \rightarrow \prod_{k=1}^K \mathbb{E} \left[ \bar{\mathbf{Z}}_k^{(1)}(t) \right], \quad K \leq M,$$

as  $t \rightarrow \infty$ .

In particular, this result says that as  $t \rightarrow \infty$ ,

$$\text{Cov}(\bar{\mathbf{Z}}_k^{(1)}(t), \bar{\mathbf{Z}}_s^{(1)}(t)) \rightarrow 0$$

provided  $k \neq s$ . In Figure 5.2 we have shown this covariance as a function of time for a pair of cells evolving according to (3.2).

**5.1. Correlations in gene expression.** Let us now consider a specific example of a network that does not satisfy the above corollary, but satisfies the hypothesis of Theorem 4.2, namely, the gene network of Figure 2.2. It turns out this network has been well studied from the perspective of a single cell, but not from the population perspective. In the present context,  $(x_C, x_D) = (1, 0)$  or  $(x_C, x_D) = (0, 1)$ , and for

the rate constants we will use the notation of Figure 2.2 that is typical in the gene network literature:  $\kappa_1 = \kappa_3 = \gamma$ ,  $\kappa_2 = \kappa_C$ ,  $\kappa_4 = \kappa_D$ ,  $\kappa_5 = \lambda_2$ , and  $\kappa_6 = \lambda_1$ . The PDMP (4.2) thus reduces to

$$(5.1) \quad \frac{d}{dt} \bar{Z}_A(t) = X_C(t)(\kappa_C - \gamma \bar{Z}_A(t)) + X_D(t)(\kappa_D - \gamma \bar{Z}_A(t)).$$

This particular PDMP has been well studied [23, 31, 20, 4], and one can prove the existence of, and explicitly calculate, the steady-state probability density  $\pi(z_A) = \pi(z_A, 0) + \pi(z_A, 1)$ , where  $\pi(z_A, x_C) = \lim_{t \rightarrow \infty} p(z_A, x_C, t)$  with  $p(z_A, x_C, t) dz_A = \mathbb{P}[z_A < \bar{Z}_A(t) < z_A + dz_A, X_C(t) = x_C \in \{0, 1\}]$  [23, 31]. One finds that when the switching rates  $\lambda_{1,2}$  between the active and inactive gene states are faster than the rate of degradation  $\beta$  then the steady-state density is unimodal or graded. On the other hand, if the rate of degradation is faster, then the density tends to be concentrated around  $z = 0$  or  $z = 1$ , consistent with a binary process.

For the sake of illustration, suppose that there are two cells, each containing a single copy of the gene, and that whether or not each gene is active depends on the state of the environment. Let  $\bar{Z}_j(t)$  denote the concentration of protein  $A$  produced by the gene network of the  $j$ th cell,  $j = 1, 2$ . Setting  $X_C(t) = 1 - X_D(t) = N(t) \in \{0, 1\}$ , we thus have the PDMP

$$(5.2a) \quad \frac{d}{dt} \bar{Z}_1(t) = \kappa_D + N(t)(\kappa_C - \kappa_D) - \gamma \bar{Z}_1(t),$$

$$(5.2b) \quad \frac{d}{dt} \bar{Z}_2(t) = \kappa_D + N(t)(\kappa_C - \kappa_D) - \gamma \bar{Z}_2(t).$$

For a given realization of the two-state Markov chain  $N(t)$ , we can integrate these equations to give

$$\bar{Z}_1(t) = e^{-\gamma t} \bar{Z}_1(0) + Z(t), \quad \bar{Z}_2(t) = e^{-\gamma t} \bar{Z}_2(0) + Z(t),$$

where

$$Z(t) = \int_0^t e^{-\gamma(t-s)} [\kappa_D + N(s)(\kappa_C - \kappa_D)] ds.$$

Taking the difference of these two equations shows that

$$\lim_{t \rightarrow \infty} |\bar{Z}_1(t) - \bar{Z}_2(t)| = 0,$$

so the two cells become strongly correlated with

$$\text{Cov}(\bar{Z}_1(t), \bar{Z}_2(t)) \rightarrow \text{Var}(Z(t)).$$

We will assume that the discrete process  $N(t)$  is in its stationary state so that, for example,  $\mathbb{E}[N(t)] = \rho_1$ . It then follows that

$$\mathbb{E}[\bar{Z}(t)] = \int_0^t e^{-\gamma(t-s)} [\rho_0 \kappa_D + \rho_1 \kappa_C] ds = \gamma^{-1} [\rho_0 \kappa_D + \rho_1 \kappa_C] (1 - e^{-\gamma t}),$$

where

$$\rho_0 = \frac{\lambda_2}{\lambda_1 + \lambda_2}, \quad \rho_1 = \frac{\lambda_1}{\lambda_1 + \lambda_2},$$

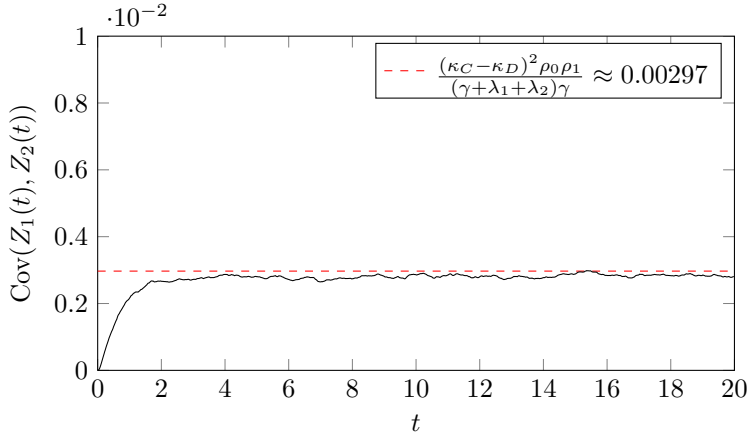


FIG. 5.3. The covariance for the population level model of (2.4) with  $M = 2$ ,  $\kappa_C = 1$ ,  $\kappa_D = 0.5$ ,  $\gamma = 1$ , and  $\lambda_1 = \lambda_2 = 10$ .

and

$$\begin{aligned}
 \text{Var}(\bar{Z}(t)) &= (\kappa_C - \kappa_D)^2 \mathbb{E} \left[ \int_0^t \int_0^t e^{-\gamma(2t-s-s')} (N(s) - \rho_1)(N(s') - \rho_1) ds' ds \right] \\
 &= (\kappa_C - \kappa_D)^2 \mathbb{E} \left[ \int_0^t \int_0^t e^{-\gamma(2t-s-s')} \text{Cov}(N(s), N(s')) ds' ds \right] \\
 &= (\kappa_C - \kappa_D)^2 \rho_0 \rho_1 \int_0^t \int_0^t e^{-\gamma(2t-s-s')} e^{-|s-s'|(\lambda_1+\lambda_2)} ds' ds \\
 &= 2(\kappa_C - \kappa_D)^2 \rho_0 \rho_1 \int_0^t \int_0^s e^{-\gamma(2t-s-s')} e^{-(s-s')(\lambda_1+\lambda_2)} ds' ds \\
 &= 2(\kappa_C - \kappa_D)^2 \rho_0 \rho_1 \frac{e^{-2\gamma t}}{\gamma + \lambda_1 + \lambda_2} \left[ \frac{e^{2\gamma t} - 1}{2\gamma} + \frac{1 - e^{\gamma - \lambda_1 - \lambda_2 t}}{\gamma - \lambda_1 - \lambda_2} \right]
 \end{aligned}$$

for  $\gamma \neq \lambda_1 + \lambda_2$ . It follows that

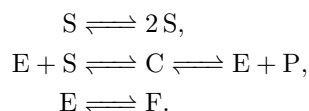
$$(5.3) \quad \text{Cov}(\bar{Z}_1(t), \bar{Z}_2(t)) \rightarrow \frac{(\kappa_C - \kappa_D)^2 \rho_0 \rho_1}{(\gamma + \lambda_1 + \lambda_2) \gamma} \neq 0.$$

A plot of this covariance as a function of time is shown in Figure 5.3. We see that after the transient phase it does converge to the predicted value.

**6. Conclusions.** In this paper we have explored how the topological deficiency relates to the stationary behavior of a multiscale CRN. The type of multiscale dynamics we have focused on is typical in systems with intrinsic and extrinsic noise [20, 28, 26, 11]. In such systems, a scaling limit of the extrinsic noise is not physically meaningful, and therefore a deterministic approximation of the full stochastic dynamics fails to capture important features of the dynamics. Instead, one must study a multiscale approximation where only the intrinsic noise is approximated deterministically [20]. One can then study the effects of extrinsic noise in isolation. Using the multiscale approximation, we have made progress toward understanding the topological features that ensure systems are robust to extrinsic noise. Our main finding is that when the deficiency of the network is zero, the multiscale approximation approaches a

deterministic fixed point almost surely. This result extends a growing body of research on the role of deficiency in stochastic CRNs, but to our knowledge, it is the only such result specifically concerning multiscale dynamics. In addition, we have shown that under certain assumptions, the multiscale approximation of a network with positive deficiency has nondeterministic behavior over long periods of time. As an application of these results, we have established conditions under which higher order statistics of a population level model vanish. These population level statistics arise when many independent chemical systems are functioning in the same random environment, and are difficult to study analytically [26, 6, 3, 4, 5].

Looking forward, it would be fruitful to extend our findings to wider classes of CRNs. Reactions satisfying Assumption 1 typically arise from model reductions of more complex reactions. For example, consider the following network, which includes an enzymatic reaction:



On the one hand, this network fails Assumption 1. On the other hand, it is clearly similar in structure to the network 3.2. From a stoichiometric perspective, the only difference is the existence of an intermediate species  $C$ . Understanding how our results can be extended to networks of this form is ongoing work. Finally, the thermodynamic implications of our results should be explored in depth. In particular, understanding which network topologies are effective at utilizing environmental energy sources is of great interest [19, 18], and our analysis suggests deficiency plays an important role in this problem.

#### REFERENCES

- [1] D. F. ANDERSON, G. CRACIUN AND T. G. KURTZ, *Product-form stationary distributions for deficiency zero chemical reaction networks*, Bull. Math. Biol., 72 (2010), pp. 1947–1970.
- [2] D. F. ANDERSON AND T. G. KURTZ, *Stochastic Analysis of Biochemical Systems*, Springer, Berlin, 2015.
- [3] P. C. BRESSLOFF, *Stochastic Fokker–Planck equation in random environments*, Phys. Rev. E, 94 (2016), 042129.
- [4] P. C. BRESSLOFF, *Stochastic switching in biology: from genotype to phenotype*, J. Phys. A, 50 (2017), 133001.
- [5] P. C. BRESSLOFF, *Stochastic Liouville equation for particles driven by dichotomous environmental noise*, Phys. Rev. E, 95 (2017), 012124.
- [6] P. C. BRESSLOFF AND S. D. LAWLEY, *Moment equations for a piecewise deterministic PDE*, J. Phys. A, 48 (2015), 105001.
- [7] D. CHATTERJEE AND D. LIBERZON, *On stability of randomly switched nonlinear systems*, IEEE Trans. Automat. Control, 52 (2007), pp. 2390–2394.
- [8] A. CHEVALLIER AND S. ENGBLOM, *Pathwise error bounds in multiscale variable splitting methods for spatial stochastic kinetics*, preprint, <https://arxiv.org/abs/1607.00805>, 2016.
- [9] D. L. COOK, A. N. GERBER, AND S. J. TAPSCOTT, *Modeling stochastic gene expression: implications for haploinsufficiency*, Proc. Natl. Acad. Sci. USA, 95 (1998), pp. 15641–15646.
- [10] A. DUNCAN, R. ERBAN, AND K. ZYGALAKIS, *Hybrid framework for the simulation of stochastic chemical kinetics*, J. Comput. Phys., 326 (2016), pp. 398–419.
- [11] M. B. ELOWITZ, A. J. LEVINE, E. D. SIGGIA, AND P. S. SWAIN, *Stochastic Gene Expression in a Single Cell*, Science, 297 (2002), pp. 1183–1186.
- [12] S. N. ETHIER AND T. G. KURTZ, *Markov processes: Characterization and convergence*, Wiley, New York, 1986.
- [13] M. FEINBERG, *Chemical reaction network structure and the stability of complex isothermal reactors I. The deficiency zero and deficiency one theorems*, Chem. Eng. Sci., 42 (1987), pp. 2229–2268.

- [14] M. FEINBERG, *The existence and uniqueness of steady states for a class of chemical reaction networks*, Arch. Ration. Mech. Anal., 132 (1995), pp. 311–370.
- [15] C. W. GARDINER, *Handbook of Stochastic Methods*, Springer, Berlin, 2009.
- [16] J. GUNAWARDENA, *Chemical Reaction Network Theory for In-Silico Biologists*, <http://vcv.med.harvard.edu/papers/crnt.pdf>, 2003.
- [17] A. HILFINGER, T. M. NORMAN, J. PAULSSON, J. YU, X. XIE, A. WRIGHT, S. JUN, X. S. XIE, N. KAMITAKI, E. M. MARTERSTECK, ET AL., *Exploiting natural fluctuations to identify kinetic mechanisms in sparsely characterized systems*, Cell Syst., 2 (2016), pp. 251–259.
- [18] J. M. HOROWITZ AND J. L. ENGLAND, *Spontaneous fine-tuning to environment in many-species chemical reaction networks*, Proc. Natl. Acad. Sci. USA, 114 (2017), pp. 7565–7570
- [19] J. M. HOROWITZ, K. ZHOU, AND J. L. ENGLAND, *Minimum energetic cost to maintain a target nonequilibrium state*, Phys. Rev. E, 95 (2017).
- [20] P. G. HUFTON, Y. T. LIN, T. GALLA, AND A. J. MCKANE, *Intrinsic noise in systems with switching environments*, Phys. Rev. E, 93 (2016), 052119.
- [21] T. JAHNKE AND M. KREIM, *Error bound for piecewise deterministic processes modeling stochastic reaction systems*, Multiscale Model. Simul., 10 (2012), pp. 1119–1147.
- [22] H.-W. KANG, T. G. KURTZ, AND L. DRIVE, *Separation of time-scales and model reduction for stochastic reaction networks*, Ann. Appl. Probab., 23 (2010), pp. 1–49.
- [23] R. KARMAKAR AND I. BOSE, *Graded and binary responses in stochastic gene expression*, Phys. Biol., 1 (2004), pp. 197–204.
- [24] T. G. KURTZ, *The relationship between stochastic and deterministic models for chemical reactions*, J. Chem. Phys., 57 (1972), pp. 2976–2978.
- [25] T. G. KURTZ, *Approximation of population processes*, CBMS-NSF Regional Conf. Ser. in Appl. Math. 36, SIAM, Philadelphia, 1981.
- [26] E. LEVIEN AND P. C. BRESSLOFF, *A stochastic hybrid framework for obtaining statistics of many random walkers in a switching environment*, Multiscale Model. Simul., 14 (2016), pp. 1417–1433.
- [27] E. LEVIEN AND P. C. BRESSLOFF, *Coupling sample paths to the thermodynamic limit in Monte Carlo estimators with applications to gene expression*, J. Comput. Phys, 346 (2017), pp. 1–13.
- [28] J. M. NEWBY, *Isolating intrinsic noise sources in a stochastic genetic switch*, Phys. Biol., 9 (2012), 026002.
- [29] M. POLETTINI, A. WACHTEL, AND M. ESPOSITO, *Dissipation in noisy chemical networks: The role of deficiency*, J. Chem. Phys., 143 (2015), 184103.
- [30] G. SHINAR AND M. FEINBERG, *Concordant chemical reaction networks*, Math. Biosci., 240 (2012) pp. 92–113.
- [31] M. W. SMILEY AND S. R. PROULX, *Gene expression dynamics in randomly varying environments*, J. Math. Biol., 61 (2010), pp. 231–251.
- [32] N. G. VAN KAMPEN, *Stochastic Processes in Physics and Chemistry*, Elsevier, 1992.